Synthesis, Activity and Durability of Pt Nanoparticles Supported on Multi-walled Carbon Nanotubes for Oxygen Reduction

Citation: Sheng, Wenchao, Seung Woo Lee, Ethan J. Crumlin, Shuo Chen, and Yang Shao-Horn. Synthesis, Activity and Durability of Pt Nanoparticles Supported on Multi-walled Carbon Nanotubes for Oxygen Reduction. Journal of The Electrochemical Society 158, no. 11 (2011): B1398. ©2011 ECS - The Electrochemical Society

As Published: http://dx.doi.org/10.1149/2.066111jes

Publisher: Electrochemical Society

Persistent URL: http://hdl.handle.net/1721.1/79085

Version: Final published version: final published article, as it appeared in a journal, conference proceedings, or other formally published context

Journal of The Electrochemical Society, **158** (11) B1398-B1404 (2011)
0013-4651/2011/158(11)/B1398/7/$28.00 © The Electrochemical Society

Synthesis, Activity and Durability of Pt Nanoparticles Supported on Multi-walled Carbon Nanotubes for Oxygen Reduction

Wenchao Sheng,[a] Seung Woo Lee,[b] Ethan J. Crumlin,[b] Shuo Chen,[b] and Yang Shao-Horn[b,c,*,z]

[a]*Department of Chemistry,* [b]*Department of Mechanical Engineering, and* [c]*Department of Material Science and Engineering, Massachusetts Institute of Technology, Cambridge, Massachusetts 02139, USA*

Carbon nanotube supported metal nanoparticles (NPs) have attracted considerable attention due to their great potential for heterogeneous catalysis. In this paper, surfactant-free and well dispersed platinum (Pt) NPs supported on multi-walled carbon nanotubes (MWCNTs) were synthesized by immobilization of negatively charged Pt precursor ($PtCl_4^{2-}$) onto positively charged MWCNTs (NH_3^+-MWCNTs) by electrostatic interactions, which was reduced subsequently to Pt NPs of ∼2 nm supported on MWCNTs by heating in 4% H_2 atmosphere. The Pt loading on MWCNTs could be controlled by the pH of the suspension of Pt precursor and MWCNTs, and the Pt-precursor concentration in the suspension. These Pt NPs supported on MWCNTs showed comparable oxygen reduction reaction (ORR) activity to a commercial Pt catalyst supported on high-surface-area carbon but with enhanced durability.
 [DOI: 10.1149/2.066111jes]

Manuscript submitted June 6, 2011; revised manuscript received August 18, 2011. Published October 5, 2011.

Proton exchange membrane fuel cells (PEMFCs) have great potential to provide power for stationary and transportation applications.[1,2] Screening high quality catalysts in terms of activity and durability is of great importance to increase the efficiency of fuel cells, especially to promote the sluggish kinetics of oxygen reduction reaction (ORR) at the cathode.[3] Typically platinum (Pt) and Pt-based alloys shown to have the highest activities for ORR,[4,5] are made on nano-scale and supported on high-surface-area carbon (such as Ketjen) to maximize the Pt surface area per unit of mass and thus mass ORR activity for PEMFC cathode. However, a notable "cathode-thinning" effect associated with carbon corrosion can occur during the PEMFC operation,[6,7] which can lead to significant loss of the cathode void volume, electrochemically active surface area of Pt, increased mass transport resistance, and thus decreased PEMFC efficiency. For example, a carbon weight loss of 5% ∼ 8% has been shown to cause a serious current density loss of 20% ∼ 60% at 0.5 V.[8] This effect can be often observed at high cathode potentials in the range from 1.2 V to 1.5 V upon the start/stop cycles during the PEMFC operation[6,9,10] or under localized H_2 starvation conditions[9,11,12] as carbon corrosion rates significantly increase at such high potentials.[9] Therefore, catalyst support materials in the cathode with enhanced stability than high-surface-area carbon particles are needed to improve PEMFC performance.

One family of candidates is graphitic carbon materials such as graphene[13] and carbon nanotubes (CNTs).[14] CNTs have high electrical conductivities and high chemical stability,[15] which can be advantageous to high-surface-area carbon particles as catalyst support for PEMFC cathode. Previous studies[16,17] on the Pt nanoparticles (NPs) supported on CNTs typically show enhanced stability in comparison to those supported on Vulcan. However, the ORR specific activity of Pt NPs on multi-walled carbon nanotubes (MWCNTs) is not reported.[16,17] In this study, we report the synthesis of well-dispersed Pt NPs on MWCNTs (Pt NPs/MWCNTs) and show the specific ORR activity of Pt NPs/MWCNTs comparable to a state-of-the-art commercial catalyst of Pt NPs supported on high-surface-area carbon. Here we employ electrostatic interactions between negatively charged Pt precursor and positively charged amine functional groups on MWCNTs to anchor Pt-containing species on MWCNTs. Conventional methods to prepare metal NPs/CNTs such as 1) direct decoration of pre-synthesized metal NPs onto CNTs;[18–20] 2) electrodeposition of dissolved metal precursors in aqueous solution onto CNTs;[21,22] and 3) chemical reduction of metal precursors using a reducing reagent such as supercritical methanol,[23] copper foil,[24] or CNT itself,[25] often result in NP agglomeration, poor particle size distributions, and particle surface contamination/poisoning. Recent studies[26,27] have shown that anchoring negatively charged Pt-containing species such as hexachloroplatinate (IV) anions in the Pt precursor on positively charged MWCNTs by electrostatic interactions, which is followed by chemical reduction, can produce well-dispersed Pt NPs on MWCNTs. Unlike these previous studies,[26,27] neither polymers nor surfactants are used to create surface charges on MWCNTs in this study. In addition, a high-temperature H_2 reduction step (Fig. 1) is employed to generate highly dispersed, poisoning-free Pt NPs of ∼2 nm on MWCNTs instead of chemical solution reduction,[26,27] which is essential to provide high mass activity of Pt NPs as polymers, surfactants, chemical reducing agents such as ethylene glycol, and Cl^--containing Pt precursors can poison the surfaces of Pt NPs and greatly reduce the ORR activity.[28] These Pt NPs/MWCNTs catalysts exhibit higher stability against Pt surface area loss and carbon corrosion upon high potential holding at 1.5 V vs. Reversible Hydrogen Electrode (RHE) compared to that of the commercial Pt/C.

Experimental

Synthesis of Pt NPs/MWCNTs (The effects of pH and $PtCl_4^{2-}$ concentration on the loading of $PtCl_4^{2-}$ on NH_3^+-MWCNTs).— The amine functionalized MWCNTs (NH_3^+-MWCNTs) were prepared based on a method reported previously.[29] To load $PtCl_4^{2-}$ onto NH_3^+-MWCNTs, 1 mg of NH_2-MWCNTs dried at 60° C was dispersed in 3.5 mL of de-ionized water (18.2 MΩ•cm, Millipore), the pH of which was adjusted from 0 to 12 using hydrochloric acid (HCl, Sigma Aldrich) at room temperature, and measured using a pH meter (AB15plus, Sisher Scientific Inc.). 0.5 mL of K_2PtCl_4 solution was added into the NH_2-MWCNTs water suspension under stirring and the final concentration of K_2PtCl_4 in the suspension was 5 mM. The mixture was kept stirring for overnight and the final pH was recorded. Subsequently, the powder of $PtCl_4^{2-}$-adsorbed-MWCNTs ($PtCl_4^{2-}$/NH_3^+-MWCNTs) was collected through nylon membrane filter and washed several times using de-ionized water of the same pH level. To study the effect of the concentration of Pt precursor on the loading of $PtCl_4^{2-}$ on NH_3^+-MWCNTs, 1 mg of dried NH_2-MWCNTs was dispersed in 3.5 mL of de-ionized water. 0.5 mL of K_2PtCl_4 solution with different amounts of K_2PtCl_4 dissolved was added into the MWCNTs suspension under stirring, resulting in the final concentration of K_2PtCl_4 ranging from 0.1mM to 10 mM. The suspension was kept stirring for overnight, and the final pH was about 3.5. The $PtCl_4^{2-}$/NH_3^+-MWCNTs powder was collected in the same manner as mentioned above. All the experiments of loading $PtCl_4^{2-}$ onto NH_3^+-MWCNTs were carried out at room temperature. To produce Pt NPs on MWCNTs, $PtCl_4^{2-}$/NH_3^+-MWCNTs made from the suspension with a final pH of 3.5 and a final K_2PtCl_4 concentration of 5 mM were treated in 4% hydrogen (H_2) atmosphere, balanced with Argon (Ar) in an Image furnace

* Electrochemical Society Active Member.
z E-mail: shaohorn@mit.edu

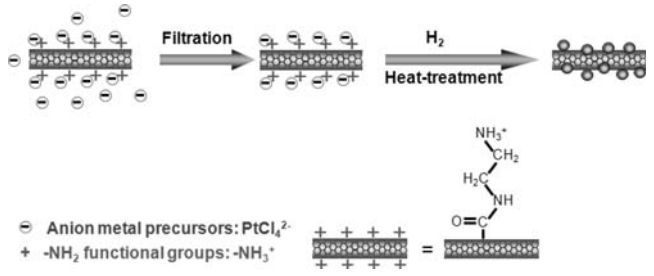

Figure 1. Synthesis route of MWCNT supported Pt NPs.

(ULVAC/SINKU-RIKO, Inc.) at 200, 300, 400, 500 or 600° C for three hours.

Physical characterization of Pt NPs/MWCNTs.— The weight loss of $PtCl_4^{2-}/NH_3^+$-MWCNTs upon heat-treatment was examined by thermal gravimetric analysis (TGA) on Netzsch STA 449 C in 2.5% H_2 atmosphere, balanced with Ar. The sweep rate was 5° C/minute. The mass loading of Pt on MWCNTs was determined by burning off MWCNTs in O_2 atmosphere. The particle sizes of Pt NPs/MWCNTs obtained at different temperatures were measured with a JEOL 2010F high-resolution transmission electron microscope (HRTEM) operated at 200 kV. TEM samples were prepared by drop-casting suspensions of Pt NPs/MWCNTs powder in ethanol on TEM grids (Lacey carbon coated copper grids, EMS), which were dried subsequently in air. At least 65 particles were measured to produce the size distribution. Surface chemical analysis of $PtCl_4^{2-}/NH_3^+$-MWCNTs in the pristine form and following heat-treatment at 200, 300, or 600° C in 4% H_2 was performed using X-ray photoemission spectroscopy (XPS) on a Kratos Axis Ultra Spectrometer (Manchester, UK) with a monochromatized aluminum X-ray source (Al Kα). High-resolution spectra were collected for the quantitative analysis of chemical compositions. All spectra were calibrated with sp^2-hybridized carbons of C 1s photoemission peak at 284.5 eV, and the photoemission spectra were fitted after a Shirley-type background subtraction. The relative sensitivity factors (RSF) values of 0.278 (Pt 4f) and 5.575 (C 1s) were supplied by the XPS manufacturer (Kratos Analytical), and the peak area ratio between Pt 4f and C 1s was used for the atomic ratio quantification of Pt and C.

Electrochemical characterization of Pt NPs/MWCNTs.— The Pt NPs/MWCNTs electrodes were prepared following our previous study[30] except that Nafion binder was not used in this work. First, the powder of Pt NPs/MWCNTs was dispersed in de-ionized water (18.2 MΩ•cm, Millipore) using ultrasonication in ice-bath, generating a catalyst suspension of ∼0.5 mg/mL. Then, 15 μL of the suspension was deposited on the glassy carbon electrode (GCE) (5 mm in diameter, Pine Instrument), which was pre-polished with 0.05 micron alumna and dried in air at room temperature. Assuming the density of MWCNTs is 2 g/cm^3, the thickness of the catalyst thin film was ∼0.2 μm. As-prepared electrodes were mounted to a rotator (Pine Instruments) as the working electrode and immersed into 0.1 M perchloric acid ($HClO_4$), diluted from 70% $HClO_4$ (GFS Chemicals Inc.) with de-ionized water. A Pt wire (Pine Instrument) and a saturated calomel electrode (SCE, Analytical Sensor, Inc.) were used as the counter and the reference electrode, respectively. However, the potentials reported throughout this paper were referenced to that of the RHE, which was calibrated from the rotating disk electrode measurement of hydrogen oxidation.[30] After the electrolyte was bubbled with Ar for at least 20 minutes, the working electrode was scanned between ∼0.03 V and ∼1.1 V vs. RHE at a sweep rate of 50 mV/s for ∼60 cycles till reaching the steady state. The cyclic voltammograms (CVs) were then recorded at 50 mV/s and at the room temperature in the same potential window. The electrochemical surface area (ESA) of Pt NPs were calculated from the Pt-hydrogen underpotential deposition region between 0.05 V and ∼0.4 V vs. RHE after double layer subtraction, assuming an electrical charge density of 210 $\mu C/cm^2_{Pt}$ for one monolayer adsorption of hydrogen on Pt surface.[31] ORR activities on Pt NPs/MWCNTs and a commercial catalyst of Pt NPs supported on high-surface-area carbon (Pt/C, Tanaka Kikinzoku Kogyo, TKK) in 0.1 M $HClO_4$ were investigated using the rotating disk electrode (RDE) method. After the electrolyte was saturated with pure oxygen (O_2), ORR polarization curves were recorded between ∼0.03 V and ∼1.1 V vs. RHE at a sweep rate of 10 mV/s at room temperature and at rotation rates of 100, 400, 900 and 1600 rpm. To eliminate the background contribution to ORR activity, ORR currents were normalized by subtracting the corresponding CVs in Ar-saturated 0.1 M $HClO_4$ from ORR polarization currents. The kinetic current i_k of ORR without iR-correction was obtained after mass-transport correction, i.e. calculated based on the Koutecky-Levich equation, $1/i = 1/i_k + 1/i_D$, where i is the measured current, i_D is diffusion-limited current. Normalization of the kinetic current i_k by the ESA of Pt from CVs provided the specific activity i_s, and i_s at 0.9 V vs. RHE was used to compare the catalytic properties among the samples. The Koutecky-Levich plot ($1/i \propto 1/\omega^{1/2}$) from $1/i = 1/i_k + 1/i_D = 1/i_k + 1/Bc_0\omega^{1/2}$ was obtained at E = 0.6 V. In the Levich equation, $Bc_0 = 0.2nFC_{O_2}(D_{O_2})^{2/3}\nu^{-1/6}$ where n is the apparent number of electrons transferred in the reaction, F is Faraday's constant, C_{O_2} is the O_2 concentration in 0.1 M $HClO_4$ (1.26×10^{-3} molL^{-1}), D_{O_2} is the diffusivity of O_2 in dilute electrolyte solutions (1.93×10^{-5} cm^{2}s^{-1}) and ν is the kinematic viscosity of the electrolyte (1.009×10^{-2}cm^{2}s^{-1}).[32] To compare the durability of Pt NPs/MWCNTs and Pt/C, potential holding experiments were performed in Ar-saturated 0.1 M $HClO_4$ at 0.5, 1.2 and 1.5 V vs. RHE at room temperature. After holding the working electrode at these potentials for a certain period of time (up to 36 hours), CVs of Pt NPs/MWCNTs and Pt/C were collected at 50 mV/s at room

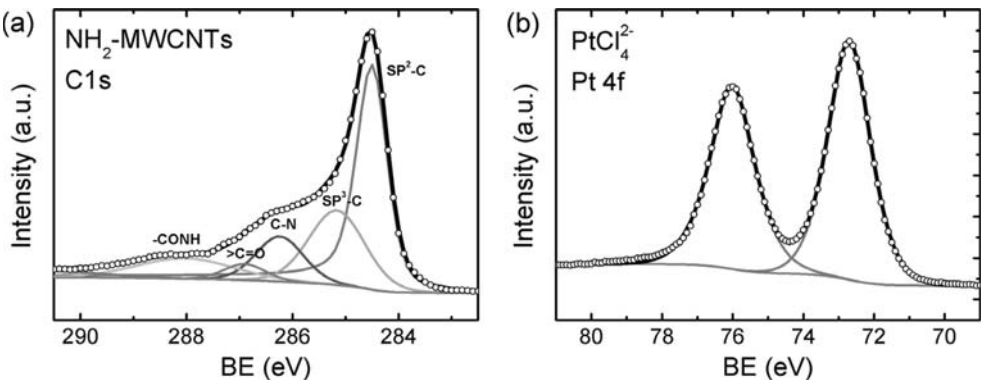

Figure 2. Representative XPS spectra of $PtCl_4^{2-}/NH_3^+$-MWCNTs: (a) C 1s; and (b) Pt 4f. Curve-fitting has been made according to reference 29 after a Shirley-type background subtraction, and all spectra have been calibrated to sp^2 hybrid carbon at 284.5 eV.

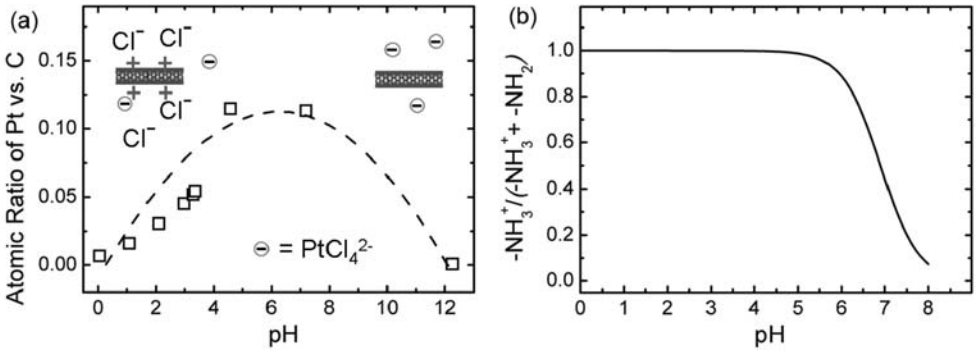

Figure 3. (a) Change of atomic ratio between Pt and C with the pH of suspensions containing $PtCl_4^{2-}$ and NH_2-MWCNTs. The concentration of $PtCl_4^{2-}$ is fixed at 5 mM; (b) Simulated fraction of protonated amines among the total amine functional groups at different pH based on $pK_a = pH - \log[-NH_2]/[-NH_3^+]$, assuming that amine functionalized MWCNTs have a same pK_a (~6.9) as that of $^+NH_3(CH_2)_2NH_3^+$.

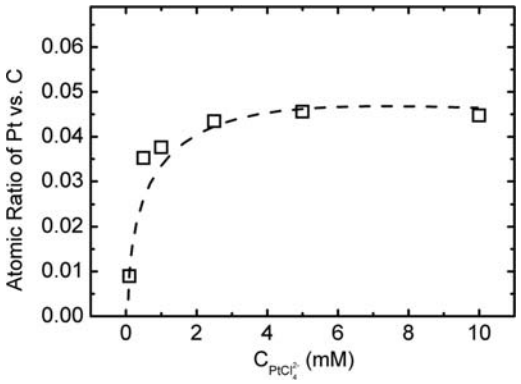

Figure 4. Change of atomic ratio between Pt and C with the concentration of $PtCl_4^{2-}$ in suspensions. The pH of the suspensions is about 3.5. The total volume of the suspension is 4 mL.

temperature, and the Pt-H underpotential deposition region was used to calculate the true ESA of Pt and then plotted as a function of holding time.

Results and Discussion

XPS results of $PtCl_4^{2-}/NH_3^+$-MWCNTs and Pt NPs/MWCNTs.— The C 1s and Pt 4f peak regions of $PtCl_4^{2-}/NH_3^+$-MWCNTs are shown in Figs. 2a and 2b, respectively. In addition to the sp^2 and sp^3 C peaks, several oxidized components associated with surface functional groups similar to those reported previously[29] were observed. Pt 4f doublets, Pt $4f_{7/2}$ and Pt $4f_{5/2}$, were found to have binding energy of 72.7 eV and 76.0 eV, respectively, which agrees well with previously reported 73.2 eV of Pt $4f_{7/2}$ for K_2PtCl_4,[33] presumably corresponding to $PtCl_4^{2-}$ species on MWCNTs. The influence of suspension pH on the atomic ratio between Pt and C is shown in Fig. 3a, where both strong basic and strong acidic suspensions result in a very low $PtCl_4^{2-}$ loading and pH values of 5 ~ 8 show the maximum loading of Pt on MWCNTs. The low Pt loading at pH = 12 in Fig. 3a can be attributed to reduced electrostatic interactions between NH_2-MWCNTs and $PtCl_4^{2-}$ as the amine functional groups on MWCNTs gradually become un-protonated ($-NH_2$) and the positive charge on NH_2-MWNTs decreases with increasing pH. The fraction of protonated amine $-NH_3^+$ among the total amine groups was estimated from $pK_a = pH - \log[-NH_2]/[-NH_3^+]$. Assuming the amine functional groups on MWCNTs have the same pK_a value (~6.9)[34] as $^+NH_3$-(CH_2CH_2)-NH_3^+, the $-NH_3^+$ fraction was found to stay constant up to a pH of ~5 but decrease rapidly at pHs greater than 5 (Fig. 3b), which is in agreement with nearly no Pt found at pH = 12 (Fig. 3a). However, the gradual reduction of Pt loading on MWCNTs with decreasing pH at pHs lower than 5 (Fig. 3a) cannot be explained by reduced electrostatic interactions between NH_2-MWCNTs and $PtCl_4^{2-}$. On the other hand, competitive adsorption of Cl^- to $PtCl_4^{2-}$ started to dominate, which was introduced when hydrochloric acid was added to lower the pH value. Considering the concentration of $PtCl_4^{2-}$ of 5 mM used in this study, the concentration of Cl^- was approximately twice that of $PtCl_4^{2-}$ at pH = 2, where the electrostatic interactions between $-NH_3^+$ and Cl^- could screen effective adsorption of $PtCl_4^{2-}$ and reduce Pt loading onto MWCNTs at low pHs.

The concentration of Pt precursor also influenced the Pt loading on MWCNTs, as shown in Fig. 4, which was found to increase as the concentration of Pt precursor increased, and eventually reach a plateau at or greater than ~1 mM of $PtCl_4^{2-}$. It is proposed that at or greater than 1 mM of $[PtCl_4^{2-}]$, the number of $-NH_3^+$ functional

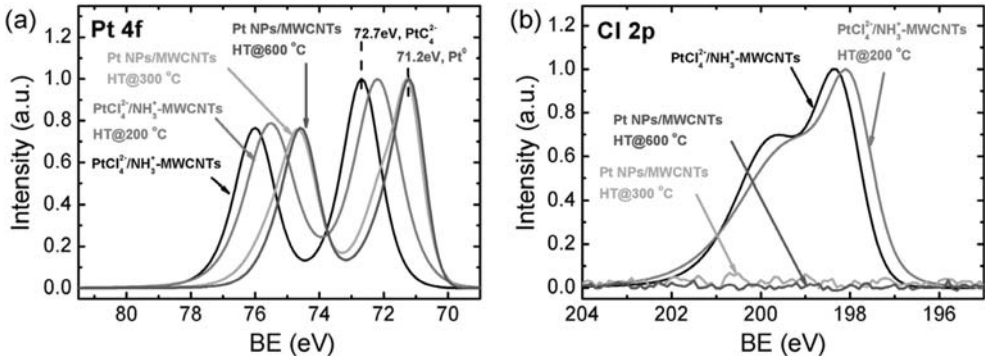

Figure 5. XPS spectra of $PtCl_4^{2-}/NH_3^+$-MWCNTs upon heat-treatment in 4% H_2 for (a) Pt 4f; and (b) Cl 2p.

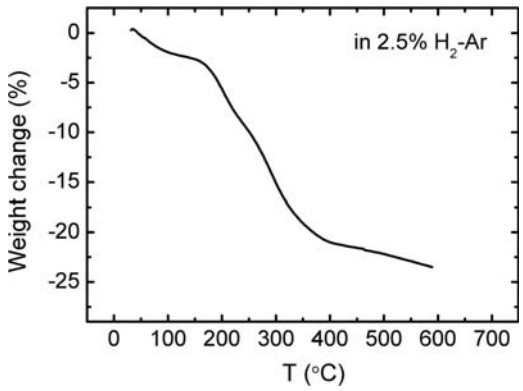

Figure 6. Weight change of $PtCl_4^{2-}$/ NH_3^+-MWCNTs upon heat-treatment in 2.5% H_2. The sweep rate is 5° C/minutes.

groups available on MWCNTs limits the adsorption of $PtCl_4^{2-}$ on MWCNTs (nominally 2 NH_3^+ for one $PtCl_4^{2-}$). XPS analysis showed that the N/C atomic ratio of NH_2-MWCNTs was ∼0.1 in this study and previous work,[29,35] which corresponded to a maximum number of ∼4 μmoles of -NH_3^+ functional groups on 1 mg MWCNTs. If divalent $PtCl_4^{2-}$ ions were paired with a minimum number of ∼2 monovalent –NH_3^+ functional groups, the availability of NH_3^+ on MWCNTs would always limit the Pt loading on MWCNTs at or greater than 0.5 mM $PtCl_4^{2-}$ (considering 4 mL solution used, the number of $PtCl_4^{2-}$ would be 2 μmoles), which is in agreement with the observation in Fig. 4.

The Pt oxidation state change in $PtCl_4^{2-}$/NH_3^+-MWCNTs before and after heating in H_2 was investigated by XPS (Fig. 5a). Both Pt $4f_{7/2}$ and Pt $4f_{5/2}$ peaks were found to shift from binding energy of 72.7 eV and 76.0 eV for $PtCl_4^{2-}$ to lower binding energy with increasing heat-treatment temperature. Upon heating to 300° C and higher, the Pt $4f_{7/2}$ peak was detected at 71.2 eV, indicative of Pt^0,[36] where at heat-treatment temperatures lower than 300° C, Pt species on MWCNTs exhibited intermediate oxidation state between Pt(II) and Pt^0. More interestingly, heating to 300° C and higher was necessary to completely remove Cl species as evidenced by the disappearance of Cl 2p peaks (Fig. 5b), which is in agreement with complete reduction of adsorbed $PtCl_4^{2-}$ on MWCNTs to Pt^0 at 300° C and higher (Fig. 5a), and the weight loss of $PtCl_4^{2-}$/ NH_3^+-MWCNTs upon heating in H_2 from TGA measurements. As shown in Fig. 6, a considerable weight loss (∼15 wt %) was found for $PtCl_4^{2-}$/NH_3^+-MWCNTs up to ∼300° C in H_2. Considering that Pt loading was determined to be ∼21 wt% (Pt vs. Pt + NH_2-MWCNTs) by burning off MWCNTs of $PtCl_4^{2-}$/NH_3^+-MWCNTs (5 mM $PtCl_4^{2-}$) in O_2 from TGA measurements (data not shown), 1.4 μmole of Pt (5.6 μmol of Cl estimated from the Pt/Cl atomic ratio of $PtCl_4^{2-}$) were associated with 1 mg NH_2-MWCNTs. This weight loss up to ∼300° C in H_2 could be attributed mostly to the loss of Cl species (∼14 wt% estimated for complete Cl removal) and minor loss of surface functional groups on MWCNTs.

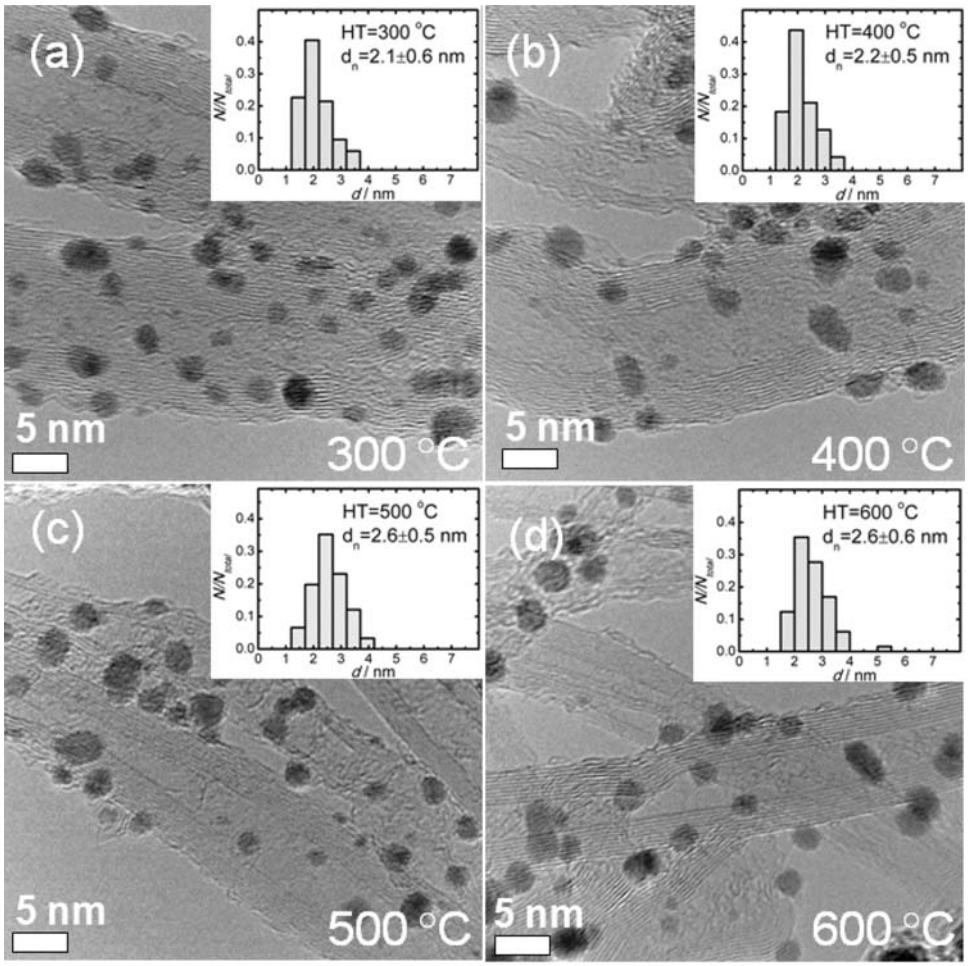

Figure 7. HRTEM images of Pt NPs/MWCNTs formed by heat-treatment of $PtCl_4^{2-}$/NH_3^+-MWCNTs at (a) 300° C; (b) 400° C; (c) 500° C and (d) 600° C. The insets are histograms of Pt NP distribution and the standard deviations are constructed based on at least 65 counts for each sample.

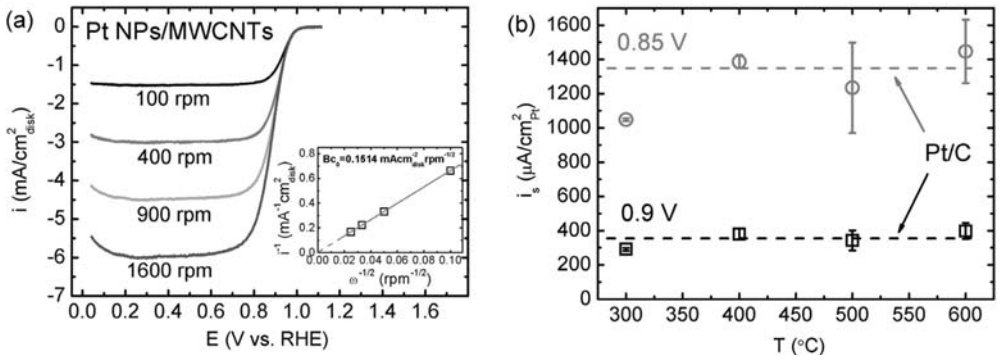

Figure 8. (a) Representative ORR polarization curves of Pt NPs/MWCNTs in O_2-saturated 0.1 M $HClO_4$, collected at 10 mV/s and at different rotating speeds. The inset is the Koutecky-Levich plot obtained at 0.6 V vs. RHE; (b) specific ORR activity at 0.9 V and 0.85 V of Pt NPs/MWCNTs treated at different temperatures, compared with those of Pt/C. The ORR tests were performed at room temperature.

HRTEM measurements revealed that Pt NPs of ∼2 nm were formed at 300° C, where Pt NPs dispersed uniformly on MWCNTs. Increasing the heat-treatment temperature to 600° C did not lead any substantial changes in particle sizes or dispersion, as shown in Figs. 7b–7d. These results clearly show that the synthesis route described in this work (Fig. 1) can produce impurity-free, well-dispersed Pt NPs on MWCNTs.

ORR activity of Pt NPs/MWCNTs.— Representative ORR polarization curves of Pt NPs/MWCNTs (treated at 600° C) at different rotation rates are shown in Fig. 8a. Following the kinetic-controlled region (above 0.95 V vs. RHE), ORR enters the kinetic-diffusion mixed controlled region (between 0.8 V and 0.95 V vs. RHE), which is limited subsequently by mass transport (below 0.8 V vs. RHE).[37,38] The Koutecky-Levich plot obtained at 0.6 V vs. RHE at different rotation rates gives a perfect line and a zero-intercept, as shown in Fig. 8a inset, showing that the RDE measurements had been performed in the thin-layer electrode regime. The slope of this plot, Bc_0, was determined to be 0.1514 $mAcm^2rpm^{-1/2}$, which suggests a four-electron transfer process of ORR.[38] ORR specific activities at 0.85 V and 0.9 V were obtained by normalizing the kinetic currents to the true ESA of Pt (110 ∼ 150 m^2/g_{Pt}), as shown in Fig. 8b. Regardless of the heat-treatment temperature, Pt NPs/MWCNTs show similar ORR specific activity (290 ∼ 400 $\mu A/cm^2_{Pt}$) at 0.9 V vs. RHE (without IR correction), which are comparable to those of the commercial Pt/C catalyst (i_s = 349 $\mu A/cm^2_{Pt}$) tested in this study. The specific ORR activity of the commercial Pt/C catalyst was higher than those reported previously.[39] This difference could be attributed to the presence of Nafion binder in the catalyst thin films in the previous work,[3] which could potentially cause catalyst agglomeration and thus reduce catalyst utilization and O_2 diffusion in the catalyst layer on GCE.

Durability of Pt NPs/MWCNTs using potential holding experiments.— CVs of Pt NPs/MWCNTs and commercial Pt/C

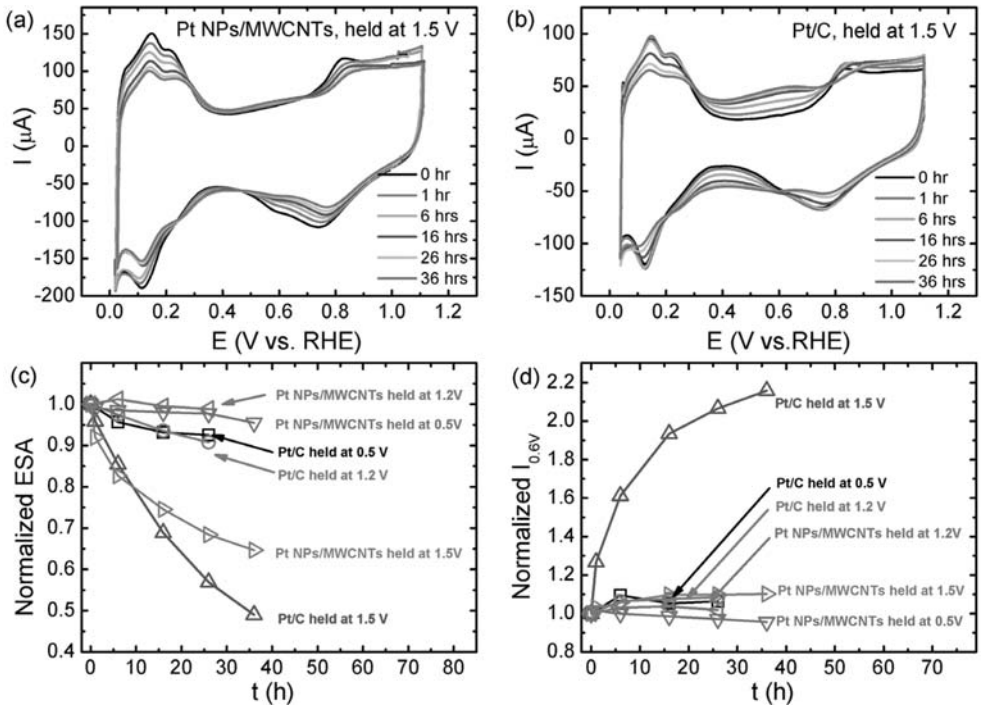

Figure 9. (a) Cyclic voltammograms (CVs) collected in Ar-saturated 0.1 M $HClO_4$ after potential holding at 1.5 V vs. RHE for a period of time for (a): Pt NPs/MWCNTs; and (b) Pt/C. The CVs were obtained at a scanning rate of 50 mV/s at room temperature. (c) Normalized electrochemical surface areas of Pt NPs/MWCNTs and Pt/C upon potential holding; and (d) Normalized double-layer currents at 0.6 V vs. RHE of Pt NPs/MWCNTs and Pt/C upon potential holding.

as a function of holding time at 1.5 V vs. RHE are shown in Figs. 9a and 9b, respectively, where such a high voltage was used to specifically examine the stability of carbon support. The CVs present a Pt-H adsorption/desorption region (below ∼0.4 V vs. RHE), a double layer region (between 0.4 V and 0.6 V vs. RHE) and Pt-OH interaction region (above 0.6 V vs. RHE).[39,40] Both Pt NPs/MWCNTs and Pt/C show current reduction in the Pt-H adsorption/desorption region with increasing time at 1.5 V vs. RHE. The Pt ESAs determined from the Pt-H region of Pt NPs/MWCNTs and Pt/C revealed that the Pt ESA loss was significant for both, and that for Pt/C (55%) was somewhat larger than Pt NPs/MWCNTs (35%) after 36 hours, as shown in Fig. 9c. This is in contrast to much less ESA loss upon potential holding at lower voltages such as 0.5 V and 1.2 V vs. RHE (Fig. 9c). The ESA loss of Pt NPs/MWCNTs and Pt/C after potential holding at 1.5 V vs. RHE was associated with significant Pt NP growth, as evidenced from HRTEM images in Figs. 10a and 10b, respectively. Particle growth is a typical consequence of Pt dissolution/redeposition (also known as Ostwald ripening) or coalescence via crystal migration.[41] Previous study[42] has shown that Ostwald ripening is a main mechanism during durability test at low potential region (0.6 ∼ 1.0 V vs. RHE). However, Ostwald ripening usually involves dissolution of Pt at high potentials and reduction at lower potentials, which could not be achieved during static potential holding measurements. In addition, Pt dissolution at 1.5 V is inhibited due to the passivation of Pt oxides,[43] suggesting that coalescence via crystal migration instead of Ostwald ripening is a mechanism at high potential holding condition (>1.2 V vs. RHE). Interestingly, after potential holding, both single crystal and polycrystal worm-like Pt NPs on the order of 10 nm were observed, which is in agreement with previous study,[44] where the particle growth has been attributed to Pt NP migration and coalescence on carbon.[41]

MWCNTs in Pt NPs/MWCNTs appeared to be more stable against oxidation, as evidenced by the fact that the double layer current of Pt NPs/MWCNTs stayed nearly constant while that of Pt/C considerably increased (by 2 times) upon potential holding in 0.1 M non-adsorbing $HClO_4$ at 1.5 V vs. RHE (frequently reached upon start up/shut down cycles or local H_2 starvation) for 36 hours, as shown in Figs. 9a, 9b and 9d. The increasing double layer current shows a rectangular shape, indicative of geometric surface area increase upon potential holding, and the little reversible peak at 0.6 V can be attributed to the quinone-hydroquinone redox couple reported previously,[45] which suggests that high-surface-area carbon of commercial Pt/C was oxidized while MWCNTs were very stable during holding at 1.5 V vs. RHE. When the holding potentials were lowered to 0.5 and 1.2 V vs. RHE, no significant changes were found in the double layer current for either carbon support, as shown in Fig. 9d. This observation is consistent with previous work that shows no change in the double layer current and comparable stability against oxidation found for Pt/C (Vulcan XC-72) and Pt NPs/MWCNT held at 1.2 V vs. RHE in 0.5 M H_2SO_4 up to 192 hours,[16] which highlights potential holding at voltages greater than 1.2 V is needed in order to reveal difference in the stability between MWCNTs and carbon black against oxidation at room temperature. On the other hand, potential holding at elevated temperatures reported by Wang X. et al.[17] has shown considerably higher stability of MWCNTs against carbon oxidation relative to Vulcan XC-72 at voltages as low as 0.9 V vs. NHE in 0.5 M H_2SO_4 at 60° C. This work confirms the enhanced stability of MWCNTs relative to carbon black against oxidation, and highlights the potential of MWCNTs as a more corrosion-resistant support for PEMFC cathode.

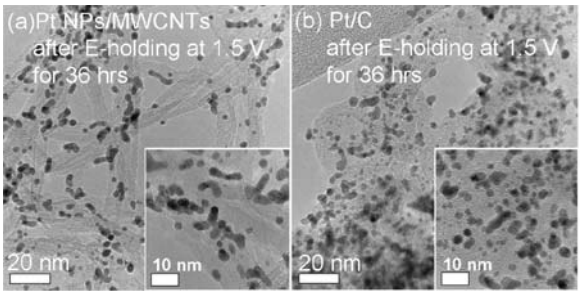

Figure 10. HRTEM images of (a) Pt NPs/MWCNTs and (b) Pt/C after potential holding at 1.5 V vs. RHE for 36 hours.

Conclusions

We have demonstrated a simple approach to synthesize well-dispersed, Cl-free Pt NPs of ∼2 nm supported on MWCNTs by H_2 reduction of $PtCl_4^{2-}/NH_3^+$-MWCNTs at temperatures greater than 300° C. Pt NPs/MWCNTs show comparable specific ORR activity (0.3 ∼ 0.4 mA/cm^2_{Pt} at 0.9 V vs. RHE) to that of a state-of-the-art commercial catalyst with Pt NPs supported on high-surface–area carbon. In addition, Pt NPs/MWCNTs exhibit considerably less Pt surface area loss, which most likely results from Pt NP migration and coalescence on carbon support, and enhanced stability against carbon oxidation relative to commercial Pt/C upon potential holding up to 1.5 V vs. RHE.

Acknowledgments

The authors would like to thank Dr. Surendra Singh for the assistance for TGA measurements at Exponent Inc. S.W.L. acknowledges a Samsung Scholarship from the Samsung Foundation of Culture. This work was supported in part by the DOE Hydrogen Initiative program under award number DE-FG02-05ER15728 and the U.S. Department of Energy, Office of Energy Efficiency and Renewable Energy, Fuel Cell Technologies Program through Argonne National Laboratory under contract DE-AC02-06CH11357. This research made use of the Shared Experimental Facilities supported by the MRSEC Program of the National Science Foundation under award number DMR-08-19762.

References

1. F. Barbir, in *Handbook of Fuel Cells: Fundamentals, Technology and Applications*, W. Vielstich, A. Lamm, H. A. Gasteiger, Editor, Vol. 4, John Wiley & Sons, New York (2003).
2. G. Konrad, M. Sommer, B. Loschko, A. Schell, and A. Docter, in *Handbook of Fuel Cells: Fundamentals, Technology and Applications*, W. Vielstich, A. Lamm, H. A. Gasteiger, Editor, Vol. 2, John Wiley & Sons, New York (2003).
3. H. A. Gasteiger, S. S. Kocha, B. Sompalli and F. T. Wagner, *Applied Catalysis B-Environmental*, **56**, 9–35 (2005).
4. V. Stamenkovic, B. S. Mun, K. J. J. Mayrhofer, P. N. Ross, N. M. Markovic, J. Rossmeisl, J. Greeley, and J. K. Norskov, *Angewandte Chemie-International Edition*, **45**, 2897–2901 (2006).
5. V. R. Stamenkovic, B. Fowler, B. S. Mun, G. F. Wang, P. N. Ross, C. A. Lucas, and N. M. Markovic, *Science*, **315**, 493–497 (2007).
6. C. A. Reiser, L. Bregoli, T. W. Patterson, J. S. Yi, J. D.L. Yang, M. L. Perry, and T. D. Jarvi, *Electrochemical and Solid State Letters*, **8**, A273–A276 (2005).
7. J. X. Zhang, B. A. Litteer, W. Gu, H. Liu, and H. A. Gasteiger, *Journal of the Electrochemical Society*, **154**, B1006–B1011 (2007).
8. H. A. Gasteiger, W. Gu, B. Litteer, R. Makharia, B. Brady, M. Budnski, E. Thompson, F. T. Wagner, S. G. Yan, and P. T. Yu, *Mini-Micro Fuel Cells: Fundamentals and Applications*, 225–233 (2008).
9. R. Makharia, S. S. Kocha, P. T. Yu, M. A. Sweikart, W. Gu, F. T. Wagner, and H. A. Gasteiger, *ECS Transactions*, **1**, 3–18 (2006).
10. P. T. Yu, W. Gu, R. Makharia, F. T. Wagner, and H. A. Gasteiger, *ECS Transactions*, **3**, 797–809 (2006).
11. Z. Y. Liu, B. K. Brady, R. N. Carter, B. Litteer, M. Budinski, J. K. Hyun and D. A. Muller, *Journal of the Electrochemical Society*, **155**, B979–B984 (2008).
12. T. W. Patterson and R. M. Darling, *Electrochemical and Solid State Letters*, **9**, A183–A185 (2006).
13. Y. Y. Shao, S. Zhang, C. M. Wang, Z. M. Nie, J. Liu, Y. Wang, and Y. H. Lin, *Journal of Power Sources*, **195**, 4600–4605 (2010).
14. R. Borup, J. Meyers, B. Pivovar, Y. S. Kim, R. Mukundan, N. Garland, D. Myers, M. Wilson, F. Garzon, D. Wood, P. Zelenay, K. More, K. Stroh, T. Zawodzinski, J. Boncella, J. E. McGrath, M. Inaba, K. Miyatake, M. Hori, K. Ota, Z. Ogumi, S. Miyata, A. Nishikata, Z. Siroma, Y. Uchimoto, K. Yasuda, K. I. Kimijima, and N. Iwashita, *Chemical Reviews*, **107**, 3904–3951 (2007).
15. M. Endo, M. S. Strano, and P. M. Ajayan, *Carbon Nanotubes*, **111**, 13–61 (2008).
16. Y. Y. Shao, G. P. Yin, Y. Z. Gao and P. F. Shi, *Journal of the Electrochemical Society*, **153**, A1093–A1097 (2006).

17. X. Wang, W. Z. Li, Z. W. Chen, M. Waje, and Y. S. Yan, *Journal of Power Sources*, **158**, 154–159 (2006).
18. E. Unger, G. S. Duesberg, M. Liebau, A. P. Graham, R. Seidel, F. Kreupl, and W. Hoenlein, *Applied Physics a-Materials Science & Processing*, **77**, 735–738 (2003).
19. A. Kongkanand, S. Kuwabata, G. Girishkumar, and P. Kamat, *Langmuir*, **22**, 2392–2396 (2006).
20. S. J. Henley, P. C. P. Watts, N. Mureau, and S. R. P. Silva, *Applied Physics a-Materials Science & Processing*, **93**, 875–879 (2008).
21. T. M. Day, P. R. Unwin, and J. V. Macpherson, *Nano Letters*, **7**, 51–57 (2007).
22. B. M. Quinn, C. Dekker, and S. G. Lemay, *Journal of the American Chemical Society*, **127**, 6146–6147 (2005).
23. Z. Y. Sun, L. Fu, Z. M. Liu, B. X. Han, Y. Q. Liu, and J. M. Du, *Journal of Nanoscience and Nanotechnology*, **6**, 691–697 (2006).
24. L. T. Qu, L. M. Dai, and E. Osawa, *Journal of the American Chemical Society*, **128**, 5523–5532 (2006).
25. H. C. Choi, M. Shim, S. Bangsaruntip, and H. J. Dai, *Journal of the American Chemical Society*, **124**, 9058–9059 (2002).
26. S. J. Guo, S. J. Dong, and E. K. Wang, *Advanced Materials*, **22**, 1269–1272 (2010).
27. S. Wang, S. P. Jiang, and X. Wang, *Nanotechnology*, **19**, 5601–5606 (2008).
28. N. M. Markovic and P. N. Ross, *Surface Science Reports*, **45**, 121–229 (2002).
29. S. W. Lee, B. S. Kim, S. Chen, Y. Shao-Horn, and P. T. Hammond, *Journal of the American Chemical Society*, **131**, 671–679 (2009).
30. S. Chen, W. C. Sheng, N. Yabuuchi, P. J. Ferreira, L. F. Allard, and Y. Shao-Horn, *Journal of Physical Chemistry C*, **113**, 1109–1125 (2009).
31. F. C. Nart and W. Vielstich, in *Handbook of Fuel Cells: Fundamentals, Technology and Applications*, W. Vielstich, A. Lamm, and H. A. Gasteiger, Vol. 2, p. 302, John Wiley & Sons, New York (2003).
32. N. M. Markovic, H. A. Gasteiger, and P. N. Ross, *Journal of Physical Chemistry*, **99**, 3411–3415 (1995).
33. J. P. Contour, G. Mouvier, M. Hoogewys, and C. Leclere, *Journal of Catalysis*, **48**, 217–228 (1977).
34. D. H. Everett and B. R. W. Pinsent, *Proceedings of the Royal Society of London Series a-Mathematical and Physical Sciences*, **215**, 416–429 (1952).
35. S. W. Lee, N. Yabuuchi, B. M. Gallant, S. Chen, B. S. Kim, P. T. Hammond, and Y. Shao-Horn, *Nature Nanotechnology*, **5**, 531–537 (2010).
36. B. C. Beard and P. N. Ross, *Journal of the Electrochemical Society*, **133**, 1839–1845 (1986).
37. K. J. J. Mayrhofer, B. B. Blizanac, M. Arenz, V. R. Stamenkovic, P. N. Ross, and N. M. Markovic, *Journal of Physical Chemistry B*, **109**, 14433–14440 (2005).
38. U. A. Paulus, A. Wokaun, G. G. Scherer, T. J. Schmidt, V. Stamenkovic, V. Radmilovic, N. M. Markovic, and P. N. Ross, *Journal of Physical Chemistry B*, **106**, 4181–4191 (2002).
39. K. J. J. Mayrhofer, D. Strmcnik, B. B. Blizanac, V. Stamenkovic, M. Arenz, and N. M. Markovic, *Electrochimica Acta*, **53**, 3181–3188 (2008).
40. J. Zhang, K. Sasaki, E. Sutter, and R. R. Adzic, *Science*, **315**, 220–222 (2007).
41. Y. Shao-Horn, W. C. Sheng, S. Chen, P. J. Ferreira, E. F. Holby, and D. Morgan, *Topics in Catalysis*, **46**, 285–305 (2007).
42. P. J. Ferreira, G. J. la O', Y. Shao-Horn, D. Morgan, R. Makharia, S. Kocha, and H. A. Gasteiger, *Journal of the Electrochemical Society*, **152**, A2256–A2271 (2005).
43. X. P. Wang, R. Kumar, and D. J. Myers, *Electrochemical and Solid State Letters*, **9**, A225–A227 (2006).
44. Y. Y. Shao, R. Kou, J. Wang, V. V. Viswanathan, J. H. Kwak, J. Liu, Y. Wang, and Y. H. Lin, *Journal of Power Sources*, **185**, 280–286 (2008).
45. K. H. Kangasniemi, D. A. Condit, and T. D. Jarvi, *Journal of the Electrochemical Society*, **151**, E125–E132 (2004).